Industrial Crops & Products 198 (2023) 116678

Contents lists available at ScienceDirect

Industrial Crops & Products

journal homepage: www.elsevier.com/locate/indcrop

Extraction and characterization of fulvic acid from corn straw compost by alkali solution acid precipitation

Meisheng Chi [a,b], Zhigang Wang [a,b,*], Weihui Xu [a,b], Ruixing Hou [c,**]

[a] College of Life Science and Agroforestry, Qiqihar University, Qiqihar 161006, China
[b] Heilongjiang Provincial Technology Innovation Center of Agromicrobial Preparation Industrialization, Qiqihar 161006, China
[c] Key Laboratory of Ecosystem Network Observation and Modelling, Institute of Geographic Sciences and Natural Resources Research, Chinese Academy of Sciences, Beijing 100101, China

ARTICLE INFO

Keywords:
Fulvic acid
Corn straw compost
Molecular model
Rice seed germination

ABSTRACT

The effective utilization of corn straw is a challenge. Extracting fulvic acid from corn straw compost improves the utilization rate of corn straw, reduces the use of chemical fertilizers, and supports sustainable agricultural development. By the response surface, the best alkali solution acid precipitation extraction conditions were obtained, which involved a KOH concentration of 9.67%, a reaction temperature of 100.32 °C, a reaction time of 9.91 h. Through the Fourier transform infrared spectroscopy (FTIR), it found that BFA contained more oxygen-containing functional groups than MFA, such as those in aliphatic, hydroxyl, ketone and carbonyl groups. Compared to the MFA, the BFA included more types of hydrogen and showed a looser superficial structure. The average molecular model of BFA was constructed with the formula $C_{17}H_{16}O_7$ (M=332). BFA has a lower molecular weight than MFA, which should ensure that BFA is readily absorbed and used by crops. BFA promoted the growth of rice seeds effectively, and the optimal BFA concentration for seed germination was 0.4%. In this study, corn straw composting was used as the main object. The molecular structure of BFA extracted from corn straw compost was established by the alkali solution acid precipitation method. It confirmed that BFA could replace MFA as a biorenewable, environmentally friendly agricultural product.

1. Introduction

During the 2021–2022 marketing year, the amount of corn (*Zea mays L.*) produced globally amounted to more than 1.2 billion metric tonnes (Statista, Inc). In the past, farmers burned the corn straw in the field because it was the cheapest and most practical way to dispose of corn straw. However, the government no longer allows open burning because it causes air pollution and fire hazards. Therefore, corn straw is composted and degraded by microorganisms to produce fulvic acid and other fertilizers, which enhances rational utilization. Composting olive waste and straw yields nitrogen-rich fulvic acid, acidic functional groups and a higher phenolic hydroxyl content (Baddi et al., 2004). Fulvic acid was extracted from pulp black liquor and was similar to the lignite fulvic acid realised through germination of rice seeds (Wang et al., 2020).

Fulvic acid is the most critical part of humic acid because it has the greatest number of oxygen—containing functional groups with the lowest molecular weight (Canellas et al., 2015). It is highly water soluble and easily absorbed by plants (Gong et al., 2022a). As a result, fulvic acid has been widely applied in many areas. In agriculture, the application of fulvic acid can improve crop yield, quality, disease resistance and resilience (Geng et al., 2020; Nargesi et al., 2022; Zhang et al., 2021). The other biological materials have been widely used in agricultural production (Riseh et al., 2021a; Pour et al., 2021; Riseh et al., 2022a; Riseh et al., 2021b; Riseh and Pour, 2021; Riseh et al., 2022b). In animal husbandry, adding fulvic acid to the diet reduces the thickness of the back fat in pigs (Chang et al., 2014) and enhances cattle growth and feed conversion rates (Cusack, 2008). In the medical field, fulvic acid has shown protective cognitive dysfunction in treatments for Alzheimer's disease (Cornejo et al., 2011). It is also used as an immunomodulator to affect the redox states of cells (Winkler and Ghosh, 2018). For environmental protection, fulvic acid can be combined with metal ions to protect the soil environment (Zang et al., 2020) and reduce the toxicities of heavy metals (Shahid et al., 2012).

The methods for extracting fulvic acid include ion exchange, sulfuric

* Corresponding author at: College of Life Science and Agroforestry, Qiqihar University, Qiqihar 161006, China.
** Corresponding author.
E-mail addresses: wangzhigang@qqhru.edu.cn (Z. Wang), hourx@igsnrr.ac.cn (R. Hou).

https://doi.org/10.1016/j.indcrop.2023.116678
Received 4 January 2023; Received in revised form 14 March 2023; Accepted 1 April 2023
Available online 12 April 2023

acid acetone, and alkali solution acid precipitation (Zhang et al., 2018a). The ion exchange is not suitable to product the fulvic acid because its operation process is complicated and costly (Zhang et al., 2018b). Because the acetone is highly toxic and fast-volatile, the sulfuric acid acetone is not recommended to use (Gong et al., 2022a; Zhang et al., 2018b). The alkali solution acid precipitation method is simple to operate and has a high yield in a short time. It also has been widely used for the extraction of fulvic acid from lignite (Huculak-Maczka et al., 2018). Recently, the chemical oxygen-based method has become a new technique for extracting fulvic acid (Gong et al., 2022a). Hydrogen peroxide, potassium permanganate, and nitric acid were used as oxidizing agents in the chemical oxygen—based method. These techniques increase fulvic acid yield and enhance the content and physiological activity of the oxygen functional groups contained in fulvic acid (Lu et al., 2021). Therefore, this study explored the effect of different oxidation methods on the extraction of BFA.

It was assumed that the functions of fulvic acid from corn straw compost (BFA) would be similar to those of MFA. To verify this theory, BFA was extracted from corn straw compost as a benchmark. Their chemical properties and biological activities were compared with those of MFA. The BFA and MFA were analysed by Fourier transform infrared spectroscopy (FTIR), ultraviolet—visible absorption spectroscopy (UV—Vis), X—ray photoelectron spectroscopy (XPS), ^{1}H nuclear magnetic resonance (^{1}H NMR), and ^{13}C nuclear magnetic resonance (^{13}C NMR). The data obtained from the characterization analyses were further explored and rice seeds were soaked to determine if the growth-promoting effect of BFA on plants was similar to that of MFA. The study provided the technical basis for managing corn straw resources as an alternative to MFA in agricultural applications.

2. Materials and methods

2.1. Materials

The MFA was purchased from Zhengzhou Qingbei Trading Co., Ltd. The corn straw compost came from Meilisi Daur District, Qiqihar City, Heilongjiang Province (123°57′34′’ E, 47°53′65′’ N). A straw decomposition agent (100-fold dilution) produced by Heilongjiang Heiwudu Biotechnology Co., Ltd. was applied. The stacking height was 2.5 m, and the water content was maintained at 60%. In the process of composting, pile aeration was performed five times, and the composting time was approximately one year. The basic physical and chemical properties are shown in Table A.1.

KOH (purity, 85%) was acquired from Tianjin Comiou Chemical Reagent Co., Ltd. H_2SO_4 (purity, 98%) was obtained from Liaoning Quanrui Reagent Co., Ltd·H_2O_2 (purity, 30%) was produced by Tianjin Kaitong Chemical Reagent Co., Ltd. The corn straw compost was dried at 70–80 °C in an oven, crushed (100 mesh), and mixed evenly.

2.2. Optimization of the extraction parameters of fulvic acid from corn straw compost

2.2.1. Single-factor experiments

First, 100 mL of deionized water, KOH (5%, 10%, 15%, 20%, and 25%) and 10 g of dried compost were added to a 250 mL beaker. Then stirring uniformly. Finally, different treatments reacted at 60 °C for 11 h. Each treatment was repeated three times. The experimental reaction temperatures and reaction times were the same as those described above. However, the reaction temperatures (20 °C, 40 °C, 60 °C, 80 °C, 100 °C) and the reaction times (7 h, 9 h, 11 h, 13 h, 15 h) were different.

When a reaction was complete, the supernatant was obtained by centrifuging at 5000 r/min for 5 min with 1 mol/L H_2SO_4 added to adjust the pH to 2. The BFA concentration was expressed in terms of the total organic carbon (TOC) content. The TOC content was determined by a carbon nitrogen analyser (Milti N/C 2100 S, Jena, Germany) (Hiradate et al., 2006; Sitnichenko et al., 2011).

2.2.2. Response surface experiments

The Box-Behnken design comprised a controlled set of experimental factors and measured responses based on one or more selection criteria. The Box—Behnken was designed with three levels: low (—1), medium (0), and high (+1). Based on the results of the single-factor experiments, the response surface experiments were designed with the Design—Expert 13 software. Ranges of the three independent variables (KOH concentration, reaction temperature, and reaction time) were used in the response surface methodology (Table A.2). The three independent variables were optimized, and 17 schemes were obtained. The specific steps of the operations were the same as those of the single-factor experiments; however, the reaction conditions were modified according to the experimental design (Table A.3).

2.3. Oxidation experiments

Fifty grams of raw material, 10% KOH, and 200 mL of deionized water were added to a 1–L beaker and stirred evenly. Air pumps (medium 8 W, Changning Co., Ltd., China) with different flow rates (6 L/min, 8 L/min, and 10 L/min) were used for oxidation. Various reaction temperatures (20 °C, 40 °C, 60 °C) and times (1 h, 3 h, 5 h) were utilized. After the reaction, the supernatant was obtained by centrifuging at 5000 r/min for 5 min with 1 mmol/L H_2SO_4 added to adjust the pH to 2. The fulvic acid content was determined with a carbon nitrogen analyser. When H_2O_2 was used in the oxidation experiments, the experimental stages were the same as the previous ones. The different features were as follows: different H_2O_2 concentrations (5%, 15%, 30%), different doses of H_2O_2 solution (10 mL, 20 mL, 30 mL), different reaction temperatures (20 ℃, 40 ℃, 60 ℃), and different reaction times (1 h, 3 h, 5 h).

2.4. Extraction and purification of potassium fulvic acid in corn straw compost

Extraction and purification of BFA substances followed the method recommended by the International Humic Substances Society, although appropriate improvements were made (Jarukas et al., 2021; Lu et al., 2021). Fifty grams of raw material, 10% KOH, and 200 mL of deionized water were added to a 500-mL beaker and stirred evenly. Then, the mixture was exposed to the environment at 20 °C for 24 h. When the reaction was complete, the supernatant was obtained by centrifuging at 5000 r/min for 5 min with 1 mol/L H_2SO_4 added to adjust the pH to 2. Then, the supernatant was dried at 65 °C in an oven (electric drying oven, GZX—9070MBE, Shanghai Bowen Industrial Co., Ltd.). The solid substance obtained after drying was potassium fulvic acid. Fulvic acid was purified as described earlier (Gong et al., 2020), except ethanol was used instead of acetone in this experiment.

2.5. Characterization of BFA and MFA

Element analyses of BFA and MFA samples were performed with an element analyser (Elementar Vario, Germany). The elements determined included C, H, S, and N. Infrared spectra were analysed in the wavenumber range 4000–400 cm^{-1} by fourier transform infrared spectroscopy (Bruker Tensor 37, Germany). The UV—Vis spectra were measured with a Lamda 35 UV spectrophotometer (Perkin Elmer company, USA), and the scan range was 200–1000 nm. Fluorescence spectra were determined with a fluorescence spectrometer (F—7000 Hitachi, Japan). The parameters were EX 200–600 nm and EM 200–600 nm, and the wavelength sweep speed was 12000 nm/min. The surface morphologies of BFA and MFA were analysed by scanning electron microscopy (SEM) with a model S 3400 (Hitachi, Japan). An ESCALAB250Xi XPS (Thermo Company) photoelectron spectrometer was used for elemental analyses and was concentrated on elements C and O. ^{1}H NMR spectra were analysed with a Fourier transform 600 MHz superconducting nuclear magnetic resonance spectrometer (AV600 BH0055, Brook, USA). The solid-state ^{13}C NMR spectra were determined with an

Advance 400 M NMR spectrometer from Bruker, Switzerland.

2.6. Establishment of the BFA molecular models

The relevant parameters for BFA molecular modelling were calculated and described in Table A.4 and Table A.5 (Gong et al., 2020).

2.7. Rice seed germination

Sprouting of the rice seeds was carried out with Dragon japonica 26 seeds. The rice seeds were disinfected with 2.5% sodium hypochlorite solution for 5 min and 75% ethanol solution for 5 min and then washed with sterile water 3–5 times until the residual solution was clean. The seeds were soaked for 24 h in 0.1%– 0.5% BFA and MFA solutions. The seeds were evenly seeded in a sterilized petri dish containing a double layer of filter paper. Each sterilized Petri dish contained twenty seeds. Each treatment was repeated three times. The seeds were cultivated in a climate chamber at 30 °C during the day and 18 °C at night. Fresh weight, root length, germination rate, and germination index were measured after culturing for ten days. The germination rate and index were calculated according to the following formulas:

$$\text{Germination rate} = \sum Gt/T \times 100\% \quad (1)$$

$$\text{Germination index} = \sum Gt/Dt^{*} \quad (2)$$

where Gt is the number of germinations on the tenth day; Dt is the corresponding germination number; and T is the total number of seeds.

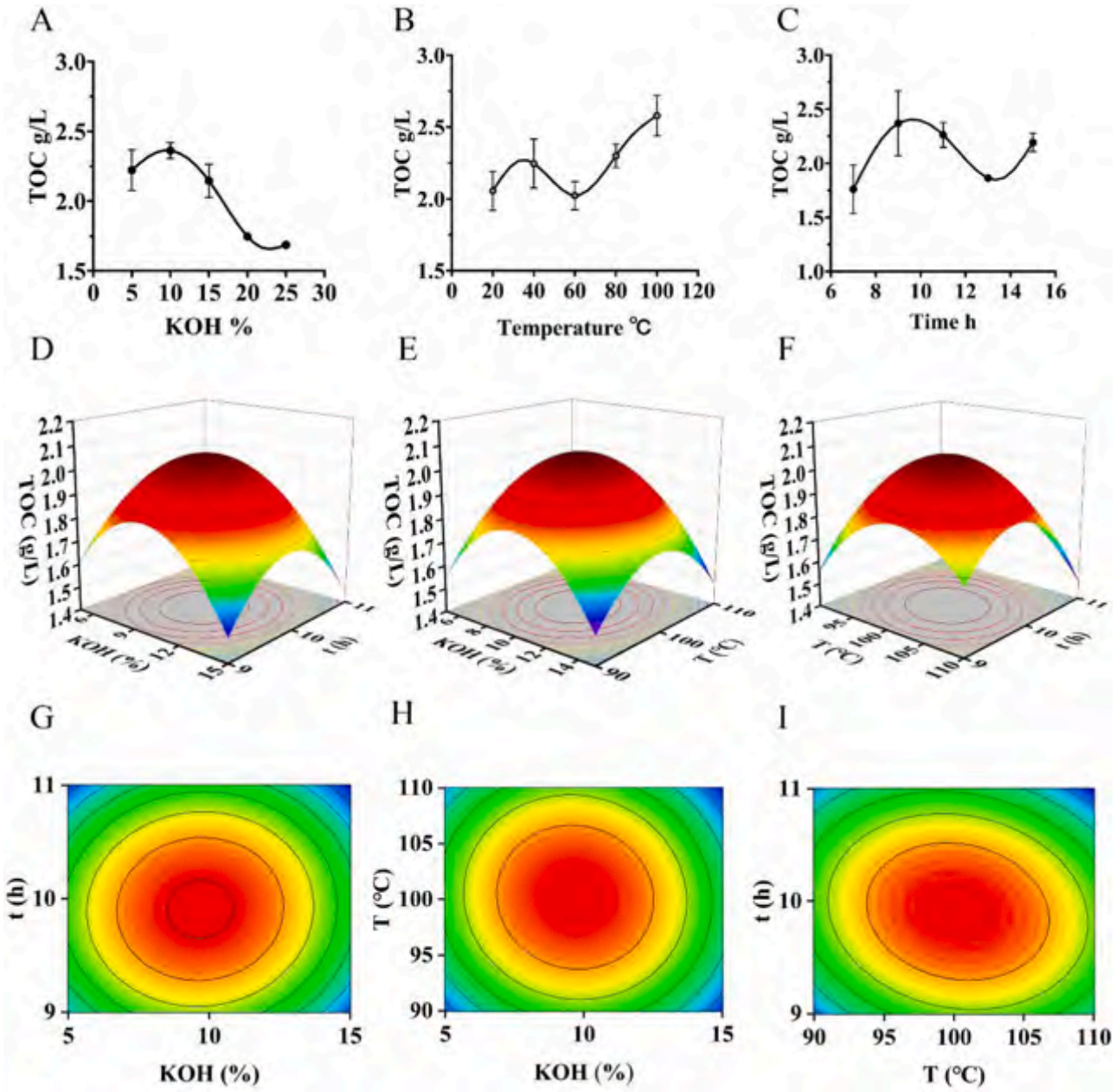

Fig. 1. Optimization of the parameters for extraction of fulvic acid from corn straw compost based on response surface experiments. A: Different KOH concentrations at 11 h and 60 ℃. B: Different reaction times at KOH concentrations of 15% and 60 ℃. C: Different reaction temperatures at KOH concentrations of 15% and 11 h. D and G: Three-dimensional interaction diagram for the KOH concentration and reaction time. E and H: Three—dimensional interaction diagram for the KOH concentration and reaction temperature. F and I: Three—dimensional interaction diagram for the reaction temperature and reaction time.

2.8. Statistical analyses

All data were analysed with SPSS 26 software (SPSS Statistics 26.0, IBM, United States). Origin 2021 (OriginLab, United States) and GraphPad Prism 8 (GraphPad Software, United States) were used to draw graphics. XPS data were fitted and analysed in detail with Peakfit V4.12. The Gaussian—Lorenz mixed fitting function was selected to obtain the binding energies and relative contents of surface elements in different oxidation states (Farzadnia et al., 2017). The spectrum was corrected with the C—C binding energy of 284.8 eV as an internal standard (Yang et al., 2019). The average values of these parameters were compared through Duncan's multiple range test at $P < 0.05$.

3. Results and discussion

3.1. Optimization of the parameters for extraction of fulvic acid from corn straw compost

When the KOH concentration was between 5% and 15%, the TOC reached a maximum (Fig. 1A). The TOC concentration increased progressively as the reaction temperature was increased (Fig. 1B). When the reaction temperature reached 100 °C, the TOC content reached a maximum. The fulvic acid extraction was optimal at 70 ℃ when using the citric acid-ethanol method (Gong et al., 2022a), which different extraction methods and raw materials might cause. As the reaction time was increased, the TOC content progressively increased (Fig. 1C), and the TOC content reached a maximum value at 9 h.

It presented a total of 17 experimental tests in the Box–Behnken, which were conducted to investigate the effects of various factors on Y (He et al., 2019). All factors influencing the inhibition efficiencies of the crystals were nonlinear. The model outcomes were statistically significant (Table A.6). The order of the effects for the three factors on the TOC concentration decreased as follows: reaction time (C) > KOH concentration (A) > reaction temperature (B). The analysis adjusted the actual equation (Eq. (3)) that used the significant terms.

$$Y\ (g/L) = 2{\cdot}060 - 0{\cdot}03625\ A + 0{\cdot}0075B - 0{\cdot}04625\ C - 0{\cdot}0225AB + 0{\cdot}01500AC - 0{\cdot}05750\ BCE - 0{\cdot}295A^2 - 0{\cdot}228B^2 - 0{\cdot}260\ C^2 \quad (3)$$

The mathematical model indicated that the optimal conditions involved a KOH concentration of 9.67%, a reaction temperature of 100.32 °C, and a reaction time of 9.91 h, and the corresponding response was 2.063 g/L. Finally, verification tests were carried out with the best culture conditions. The mean TOC concentration observed experimentally was 2.020 g/L, which was close to the model prediction of 2.063 g/L.

In the MFA extraction process, the four factors influenced the fulvic acid yield in the following order: H_2O_2 concentration, microwave power, oxygen—coal ratio, and reaction time (Gong et al., 2022a). However, this study identified reaction time as the most critical factor influencing the fulvic acid yield. A potential reason was that the extraction process varied significantly because of the different sources of raw materials.

This study used alkali solubilization acid analysis to extract the BFA from corn straw compost. It differed from MFA extraction, and specific microbial agents were utilized for composting in advance and then pulled to obtain BFA. Compared to pretreatments with HNO_3, H_3PO_4 or H_2SO_4, the method was simpler, required fewer extraction steps and yielded a high product content (Lu et al., 2021). In addition, preprocessing of the corn straw compost by microbial agents partially degraded the cellulose and other substances in the corn straw, which reduced the number of chemicals used in the extraction process and was also more suitable for the production of fulvic acid.

3.2. Oxidation experiments with fulvic acid from corn straw compost

A reaction temperature of 60 °C was optimum for H_2O_2 oxidation. The reaction temperature had no significant impact on the TOC content produced by air oxidation (Fig. 2A). A reaction time of 5 h was optimal for air oxidation, and the reaction time had no significant effect on the TOC content for H_2O_2 oxidation (Fig. 2B). Fig. 2C and D show that the best result was obtained with an air volume of 8 L/min and a H_2O_2 content at 15%. The dosage of H_2O_2 had little effect on the TOC content (Fig. E).

The fulvic acid extracted from paper mill effluents using hydrogen peroxide (H_2O_2) as an oxidizer and titanium oxide (TiO_2) as a catalyst exhibited a lower molecular weight and more functional groups (Yao et al., 2019a). The average molecular weight of the fulvic acid was decreased significantly by ozonation (Shinozuka et al., 2002). Different mechanisms may have resulted in the development of different intermediates (Li et al., 2008). Three oxidant systems (ozone, ozone-hydrogen peroxide, and catalytic ozone) decreased the content of dissolved organic carbon and biodegradable dissolved organic carbon in the fulvic acid solution (Volk et al., 1997). This indicated that oxidation was essential in extracting fulvic acid. An appropriate oxidizer may improve the performance and quality of the fulvic acid.

3.3. Characterization of BFA and MFA

3.3.1. Elemental analyses

The elemental analysis results for BFA and MFA are shown in Table 1. BFA had higher percentages of C and H than MFA, which could be because more corn straw compost dissolved into the liquid. The MFA included more sulfur content. A possible reason is that MFA was formed from the chemical reactions of plant and animal remains that took millions of years to form (Aida et al., 2022). High percentages of S and N indicated high biomolecule levels (polypeptides and polysaccharides) (Baddi et al., 2004), and these findings suggest that BFA might be more biologically active. The C/H and C/O ratios were higher in the BFA than in the MFA, indicating that the BFA components were less aromatic and had more oxygen—containing functional groups (Iimura et al., 2012). Fulvic acid isolated from the water of Ramsar Lake Mansar also had a lower percentage of N than the MFA. The C and H percentages were relatively higher than those of the MFA (Sharma and Anthal, 2022).

The total acid group content was 3.18 in MFA and 1.00 in BFA. BFA had fewer total acid groups than MFA (Table 2). Functional groups containing oxygen in BFA were predominantly acidic functional groups, including carboxylic and phenolic hydroxyl groups. The low content of acidic functional groups in BFA might be due to low humification levels (Zhang et al., 2019). The functional groups contained in fulvic acid exhibited strong complexation, chelating, and surface adsorption capacities, which reduced the loss of ammonium nitrogen (Wang et al., 2021). Fulvic acid promoted nutrient uptake in crops and enhanced the ability of crops to resist adverse environments (Lv et al., 2022). Oxygen—containing functional groups complexed Cu^{2+} in soil (Shi et al., 2018), which is beneficial for environmental protection. Fulvic acid might play an essential role in soil remediation due to its sizeable phenolic hydroxyl content (Sun et al., 2020). Fulvic acid, one of the most critical components in humic acid, contained the most oxygen-containing functional groups and had the lowest molecular weight (Gong et al., 2022a). The various extraction processes and feedstocks impact the contents of the fulvic acid functional groups (Li et al., 2013).

3.3.2. Spectral characteristics of BFA and MFA

The FTIR spectra of BFA and MFA (Fig. 3A) showed similar patterns with characteristic peaks for the major functional groups, and the FTIR spectra were consistent with the standard spectrum of fulvic acid (Yang et al., 2008). The FTIR data were compared to findings from previous studies (Gerasimowicz and Byler, 1985; Gong et al., 2020; Hernandez

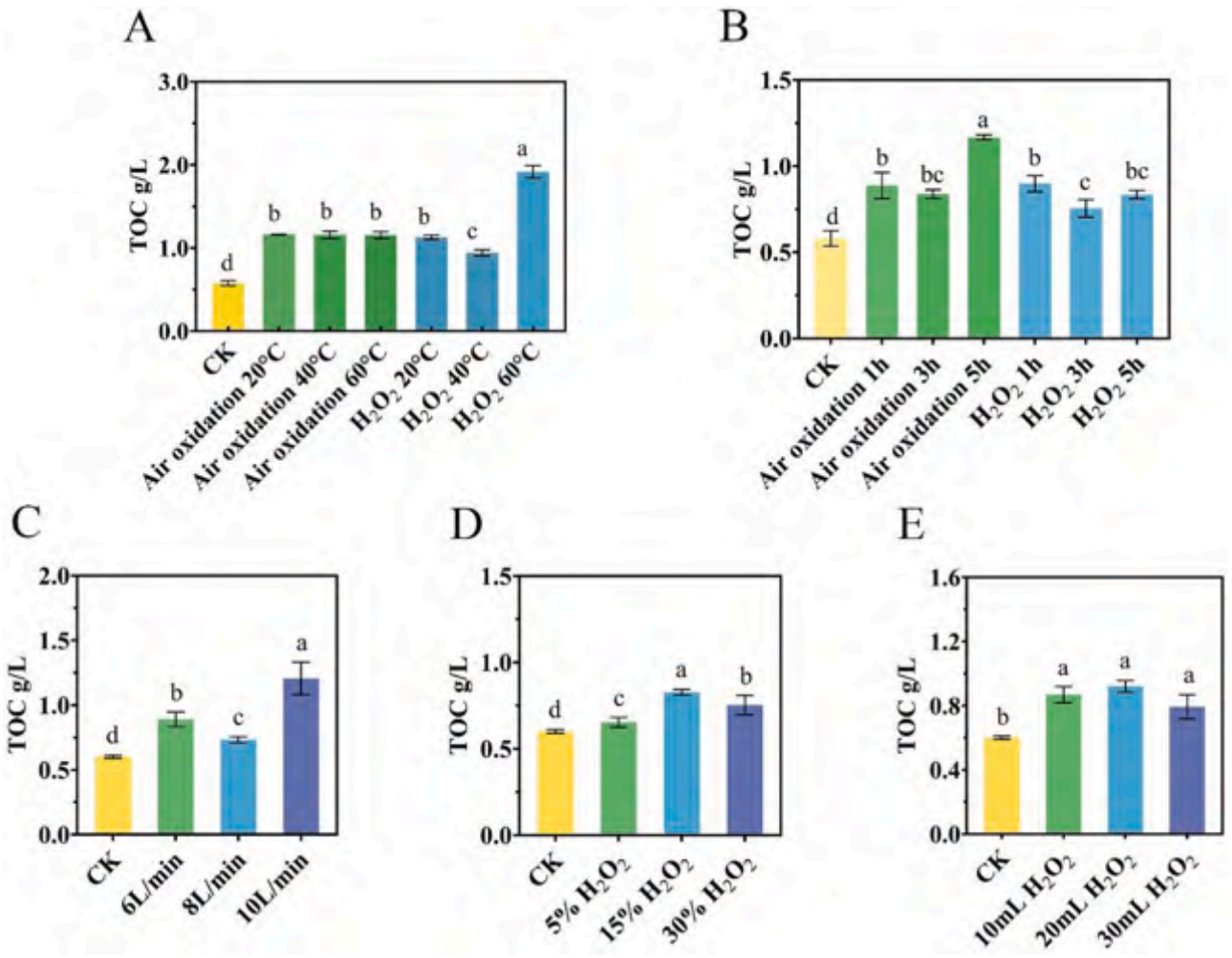

Fig. 2. Oxidation experiments with fulvic acid in corn straw compost. A: Different temperatures for the oxidation experiments with a reaction time of 3 h, an air volume of 8 L/min, and a H_2O_2 concentration of 15%. B: Different times for the oxidation experiments with a reaction temperature of 40 ℃, an air volume of 8 L/min, and a H_2O_2 concentration of 15%. C: different ventilation capacity of the oxidation experiments for a reaction time of 3 h and a reaction temperature of 40 °C. D: Different H_2O_2 concentrations for oxidation experiments with a reaction time of 3 h and reaction temperature of 40 °C. E: Different doses of H_2O_2 for the oxidation experiments with a reaction time of 3 h and a reaction temperature of 40 °C. The results are the means of three replicates with error bars showing the standard deviations. Lowercase letters represent significant differences among treatment groups.

Table 1
Elemental composition of BFA in corn straw compost and MFA in lignite.

Sample	Elemental composition							
	C (%)	N (%)	H (%)	S (%)	O (%)*	C/H	C/O	C/N
BFA	31.45	0.75	2.77.00	3.11	61.92	11.35	0.51	41.93
MFA	21.22	0.97	2.48	9.12	66.21	8.56	0.32	21.88

*This value is the result of subtraction.

Table 2
Content of acidic functional groups in BFA from corn straw compost and MFA from lignite.

Samples	Total acid group (mmol/g)	Carboxyl (mmol/g)	Phenolic hydroxyl group (mmol/g)	Phenol hydroxyl ratio (%)
BFA	1.17 ± 0.02	0.08 ± 0.01	0.93 ± 0.04	98.32 ± 0.11
MFA	3.18 ± 0.15	0.07 ± 0.02	3.13 ± 0.03	80.41 ± 0.01

et al., 1990; May, 1965). Table A.7 and Table A.8 show the peak positions and intensities of the BFA and MFA. At 1500–1000 cm^{-1}, the BFA had more peaks than MFA, which suggested that the BFA contained more stretching vibrations for C-H, C−O in hydroxyls, and C−O in phenyl ethers. The assumption has been made that microorganisms partially decomposed the organic matter during composting of the BFA (Amir et al., 2005). The BFA and MFA had a distinct strong band at 615 cm^{-1}, which was attributed to the S−O stretching vibrations of sulfonic groups. This band showed that oxidation led to the formation of sulfur-containing functional groups (Yao et al., 2019b). The BFA had more absorption bands than MFA in the region 1600 cm^{-1} – 700 cm^{-1}, which indicated that BFA had more oxygen—containing functional groups (such as hydroxyl and carboxyl groups) than MFA (Wang et al., 2020). A possible reason was that the alkyl side chains of the macromolecular structure and the methylene bonds serving as bridges were oxidized to oxygen—containing functional groups during alkaline

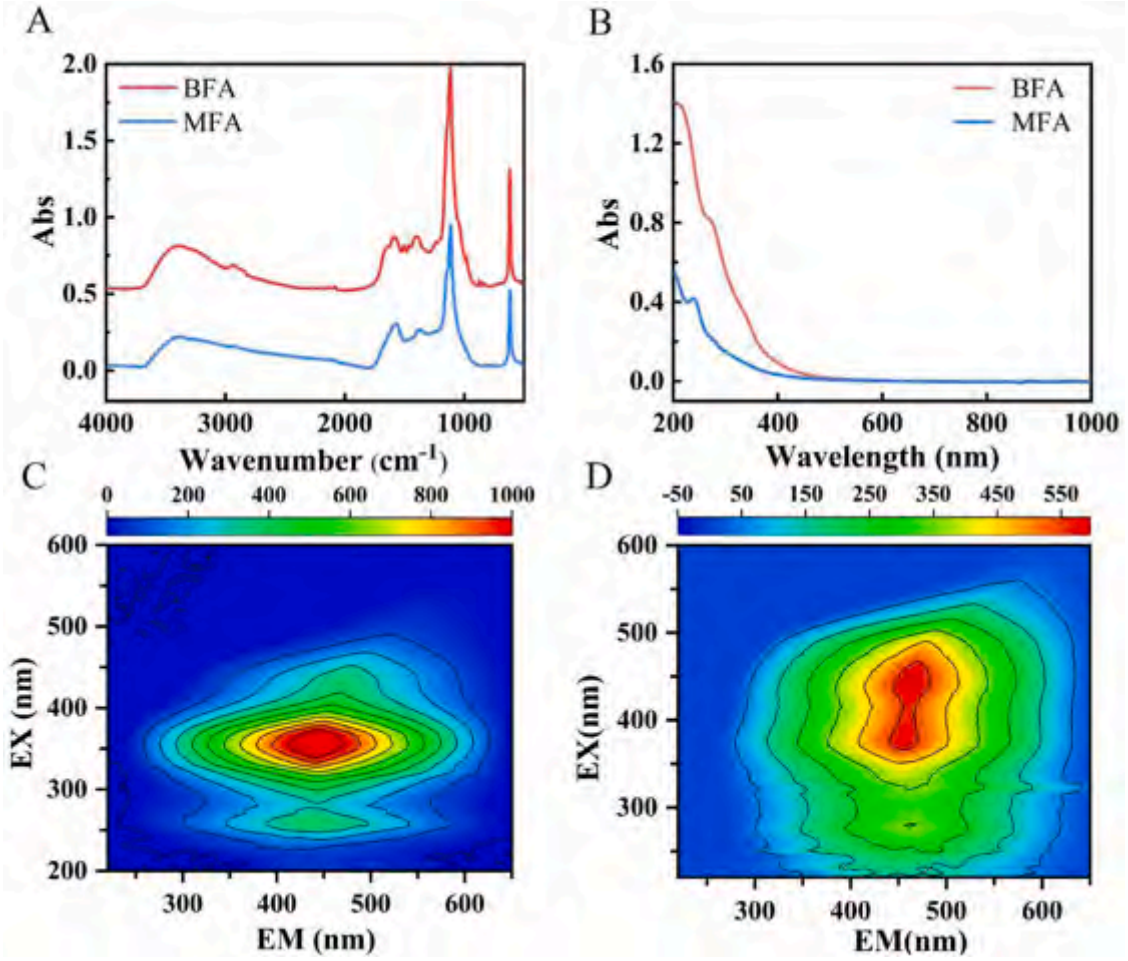

Fig. 3. Spectroscopic characterization experiments for fulvic acid from corn straw compost. FTIR spectra of BFA and MFA (A). UV—vis absorbance spectra of BFA and MFA (B). Three—dimensional excitation emission matrix fluorescence spectrum contour map for BFA and MFA (C, D).

hydrolysis of the BFA, such as carbonyls, aldehydes, and carboxylic acids (Zhang et al., 2019). Similarly, the fulvic acid derived from sewage sludge also had more oxygen-containing functional groups and fewer hydrocarbons (lower aliphatic and aromatic degrees) (Li et al., 2013; Gigliotti et al., 2001). Based on the above analyses, the FTIR data of the BFA showed many similarities with MFA in terms of spectroscopic data. However, the BFA had more hydroxide, carboxylic and small active molecular groups than MFA.

The BFA and MFA displayed similar UV—Vis spectra (Fig. 3B). Because there were many colour—generating functional groups, blue-shifts or redshifts and overlap occurred in the different absorption spectra and resulted in no pronounced absorption peaks (Zhang et al., 2019). The absorbance peak for BFA at approximately 280 nm was characteristic of double bonds (C═C, C═O and N = N) in aromatic rings or unsaturated compounds, which may exist in lignin, hydroxycinnamic acids, aniline derivatives, phenolic arenes and so on (Peuravuori and Pihlaja, 1997). Obviously, this meant that the BFA contained more aromatic rings or unsaturated compounds than the MFA. The peak strength at 230 nm for BFA and MFA indicated that the conjugated system had two double bonds in the molecule. This could come from unsaturated aldehyde or quinone groups. Previous research has shown similar results (Gong et al., 2022b). The E4/E6 ratio (the ratio of intensities for the 465–665 nm peaks) is characteristic of fulvic acid. It may represent the complexity of the molecule and the degree of conjugation for the carbonyl group (Ma et al., 2020). The E4/E6 value of the BFA was higher than that of the MFA (Table A.9), indicating that the BFA had lower aromaticity, a lower degree of carbonyl conjugation, and a smaller molecular weight. This might be one of the reasons why the BFA easy to absorb and use for crops (Zhang et al., 2021).

The three—dimensional fluorescence spectra of BFA and MFA are shown in Fig. 3C to D. The BFA had a single visible fluorescence peak located at $\lambda_{Ex/Em}$ = 335–370/440–475 nm. The MFA also had a fluorescence peak that was located at $\lambda_{Ex/Em}$ = 360–450/425–475 nm. The peaks were associated with the carboxyl and carbonyl groups (Alberts and Takacs, 2004). The complex structure of BFA is composed of a variety of groups capable of fluorescence. The overlapping of multiple peaks led to the strong intensity and wide form of the fluorescence peak. This result was consistent with the FTIR results (Fig. 3A). The fluorescence intensity of BFA was higher than that of MFA in the humic acid area, indicating that the relative concentration of humic acid in the BFA was high. The fluorescence index (FI), biological index (BIX), and humification index (HIX) were calculated to examine the characteristics of the fulvic acid (Table A.10). FI was generally used in conjunction (Gao et al., 2019; Huguet et al., 2009; Li et al., 2019). The FI of BFA was observably higher than that of MFA, indicating that it was the result of both natural and exogenous humus. The BIX of BFA (1.65) was significantly higher than that of MFA (0.45), indicating that the proportion of autogenic organic matter was high. The BFA was more conducive to crop absorption and utilization (Li et al., 2021). The HIX of MFA (10.51) was significantly higher than that of BFA (2.73), indicating that the MFA had a higher degree of organic matter humification. MFA was formed from animal and plant residues after one or more hundred million years of humification. However, the humification time for BFA was short (Aida et al., 2022), and the humification level was low.

3.3.3. Surface morphology characteristics of BFA and MFA

The SEM image of BFA showed square, irregular lamellar crystals (Fig. 4A). It was speculated that certain inorganic substances were formed during drying at a steady temperature. However, the MFA demonstrated a cluster structure (Fig. 4B). A possible reason was that MFA was extracted from lignite with a complex oxidation reduction response during the extraction process (Gong et al., 2022b). Similar results were obtained with scanning electron microscopy on fulvic acid (Jiang et al., 2011). In addition, due to the higher E4/E6 ratio, the molecular weight of MFA was smaller (Wang et al., 2015). Hence, the looser structure and smaller molecular weight of BFA were the crucial reasons for better promotion of crop growth (Li et al., 2013).

3.3.4. XPS, ^{13}C NMR and ^{1}H NMR analyses of BFA and MFA

Tables A.11 and A.12 demonstrate the XPS results for BFA and MFA. The corrected narrow C 1 s XPS data for BFA (Fig. 5A) and MFA (Fig. 5C) showed that BFA had a higher proportion of the peak at 284.82 eV. The BFA was higher than the MFA in C—C and C—H contents (Desbene et al., 1986; Farzadnia et al., 2017). Nevertheless, in the O 1 s spectra (Fig. 5B, D), there were no significant differences in the various surface compounds. This indicated that the BFA and MFA contained more C-O- and C═O (Yang et al., 2019; Gong et al., 2020). The surface compounds BFA and MFA were similar (Desbene et al., 1986). The relative contents were only partly different, which provided a theoretical basis for replacing MFA with BFA. At the same time, this result also provided a reference for further study of the mechanisms of action for BFA and MFA.

Fig. 5E–F displays the ^{1}H NMR spectra for BFA and MFA. The findings were based on a number of studies (Francioso et al., 1998; Gong et al., 2020; Javed et al., 2013; Lopez-Martinez et al., 2021; Sharma and Anthal, 2022). The observed peaks can be found in Tables A.13 (BFA) and A.14(MFA). The signals with chemical shifts from 0.8 to 4.5 ppm were partitioned into four groups: (a) aliphatic terminal methyl protons, from 0.8 to 1.4 ppm (H_1); (b) protons with polar functional groups, such as aromatic rings and carbonyl groups other than beta and beta positions in aliphatic groups, from 1.4 to 1.8 ppm (H_2); (c) protons with aromatic functional groups, such as aromatic rings and carbonyl groups in the alpha position, from 1.8 to 3.3 ppm (H_3); and (d) protons carbon—linked to heteroatoms, for instance O or N, S, etc., from 3.3 to 4.5 ppm (H_4). BFA contained more hydrogen species than MFA. The signals were mainly concentrated in the 1.8–3.3 ppm and 3.3–4.5 ppm regions. Compared to MFA, BFA had more phenol OHs with 6.27 ppm chemical shifts. This difference might be due to the different sources and extraction methods for fulvic acid (Jarukas et al., 2021; Mghaiouini et al., 2022). Based on the ^{1}H NMR results, it was estimated that the BFA contained more types of hydrogen (Sharma and Anthal, 2022). This could be a potential reason why the corn straw compost was degraded into small molecules by oxidation due to the action of microorganisms. More alcohols, aldehydes, acids, and other compounds were present in the BFA (Amir et al., 2005). Shilajit fulvic acid obtained from Shilajit capsules also showed similar results (Javed et al., 2013). The data also concurred with those reported for 1 H NMR studies on natural fulvic acid (Fujitake et al., 2012).

The CP-MAS ^{13}C solid-state NMR spectra (Fig. 5G–H) resulted in detailed distributions of C functionality and structural information for the AFB and MFA. Typical peaks for fulvic acid existed for all fulvic acids, indicating that they shared similar structural features (Martinez-Balmori et al., 2014). The results were also consistent with those of other authors (Keeler and Maciel, 2003). Among the spectra, the BFA spectrum was relatively noisy. This meant that it represented a complex mixture, while the MFA spectra were smoother, indicating that the MFA was relatively pure. These interpretations of the spectra (Table A. 15–Table A.16) were based on numerous studies (Amir et al., 2004; Baddi et al., 2004; Cao et al., 2016; Gondar et al., 2005; Inbar et al., 1992; Preston, 1996; Ricca and Severini, 1993). The total region for each spectrum was consolidated and split into the several regions: aliphatic carbon (0–50 ppm), alkyl carbon substituted by oxygen and nitrogen (50–110 ppm), aromatic carbon (110–165 ppm) and carboxyl carbon (165–200 ppm) (Table A.17). Overall, the BFA had fewer C types than the MFA. However, the BFA contained more carbohydrates than the MFA in the region between 40 and 105 ppm. Moreover, BFA contained more protonated aromatic carbons, which accounted for 50% of the total. This indicated that the BFA contained more aromatic structures. MFA contained special C types, such as amino aromatic carbons and amino aromatic carbons (Gong et al., 2020). The proportion of amino aromatic carbons in the MFA was 18.91%. Due to the high content of amino aromatic carbons, the sulfur contents in the MFA were higher than those in the BFA, which was consistent with the elemental analysis results (Table 1). All ^{13}C NMR signals for BFA and MFA matched those observed for fulvic acid by other authors (Keeler and Maciel, 2003).

In summary, MFA and BFA characterization analyses showed that there was little difference between them. The above analysis provides a theoretical basis for further explorations of BFA and its replacement by MFA.

3.4. Establishment of BFA molecular models

In this research, the molecular model was made to reveal the structural features of the BFA, with an average molecular weight under 500 amu as an example.

3.4.1. Calculation of parameters with IR and ^{13}C NMR data

Data based on elemental analysis and FTIR split-peak fitting., the calculated structural FTIR spectral parameters of BFA are as follows: I = 1.06, $f_{ar}^{H} = 0.2750$, $f_{ar} = 0.5731$, and L = 7.5510. The diverse types of carbon atoms were identified by ^{13}C NMR analyses. The ^{13}C NMR parameters of BFA are displayed in Table A.18.

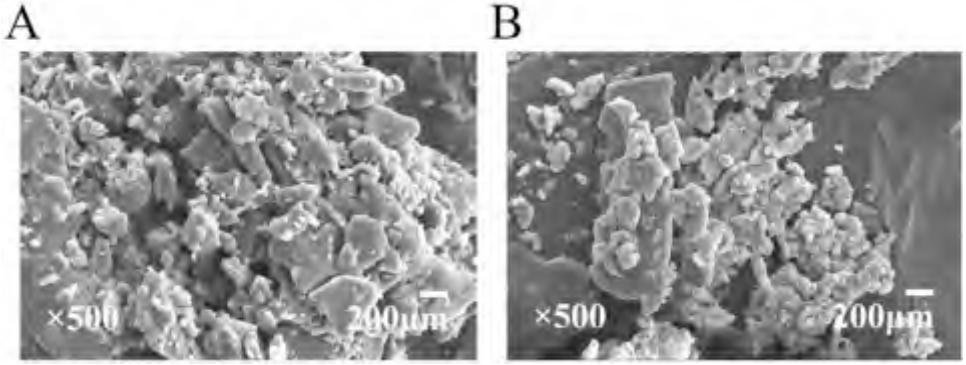

Fig. 4. Observations of the fulvic acid morphologies from corn straw compost. SEM photos of BFA (A) and MFA (B).

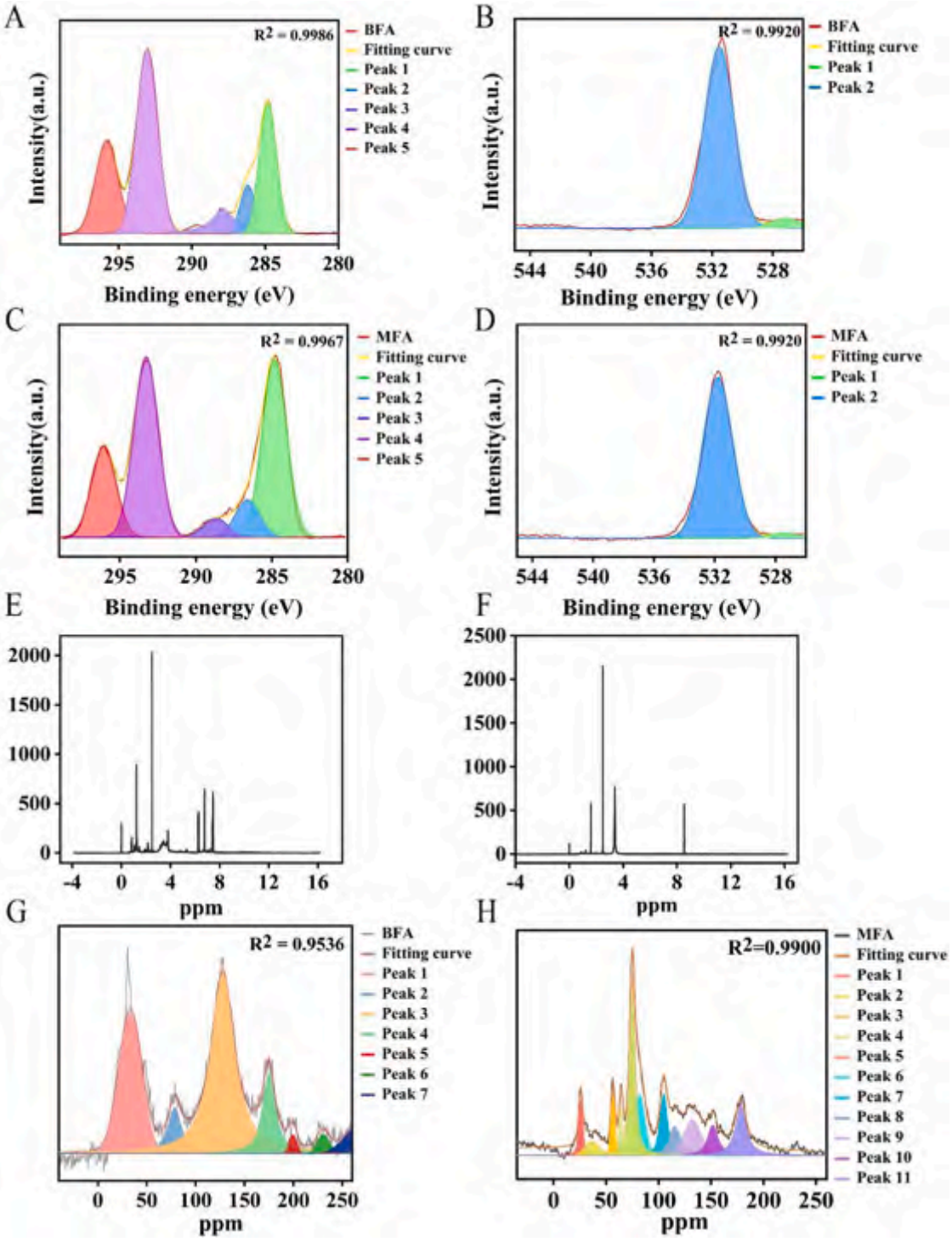

Fig. 5. Identification of the compounds on the surface in fulvic acid from corn straw compost. X-ray photoelectron spectra (XPS) and NMR spectra of BFA and MFA; C 1 s (A, C) and O 1 s (B, D) XPS data, ^{1}H NMR spectra (E, F), and ^{13}C NMR spectra (G, H).

3.4.2. Establishment and optimization of the BFA molecular structure model

Based on the elemental analysis, molecular weight, and the ^{13}C NMR (Table A.18), the average chemical formula of BFA was determined to be $C_{17}H_{16}O_7$ (Mr=332).

Based on the calculated carbon skeleton parameters, approximately 17 carbon atoms were present in benzene rings in the BFA. Therefore, two cycles of benzene were calculated in the molecular model. In BFA, the saturated aliphatic chain has five carbon atoms, the aromatic ring linked by carboxyl groups has two carbon atoms, and the methyl and methylene groups have three carbon atoms. For BFA, the molecular model consisted a phenol hydroxyl group, an aryl ether, and two carboxyl groups. With this assumption, only bit disubstituted benzene rings can be ignored in BFA. It does contain two tetrasubstituted benzene rings and one fir—substituted benzene ring.

The optimized wedge structure of BFA was obtained by quantum chemical calculations using Gaussian software, with modifying the placement and functional groups to match the experimental test data

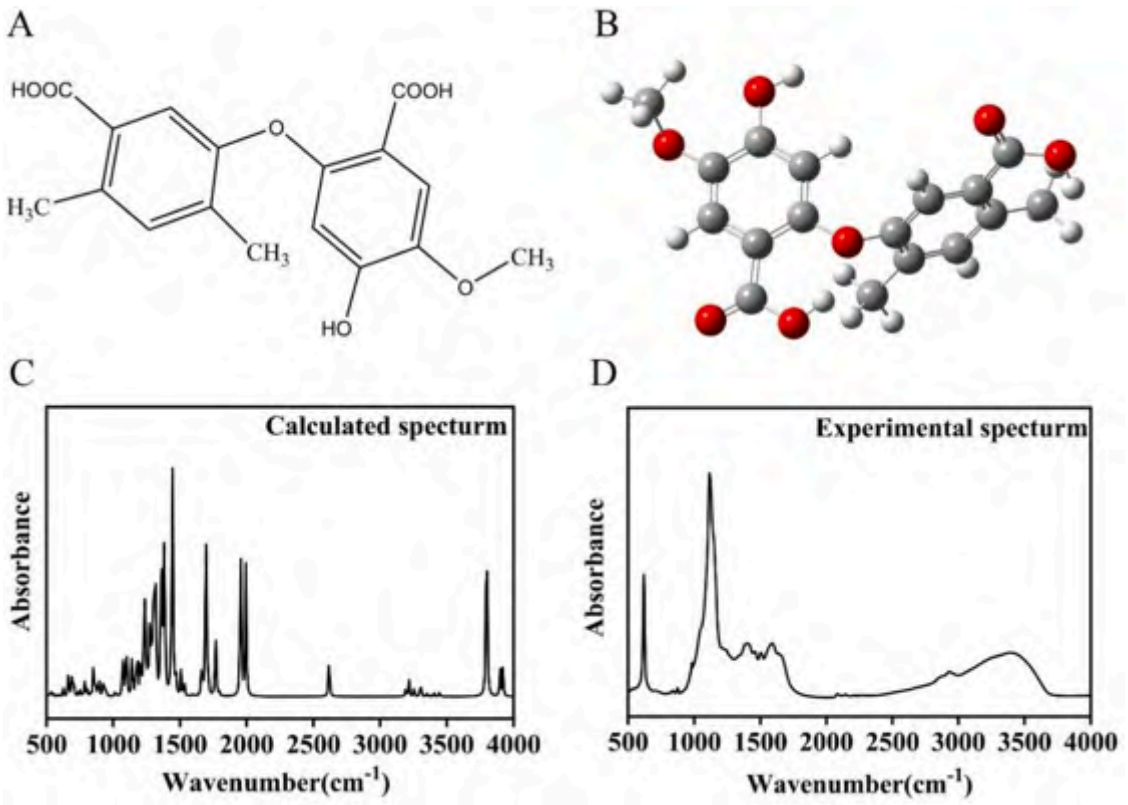

Fig. 6. Molecular model constructed for BFA. The structure of BFA (A). The ball—and—stick model of BFA (red spheres: oxygen atoms; grey spheres: carbon atoms; white spheres: hydrogen atoms) (B). Comparison of the experimental and calculated spectra for BFA (C-D).

(Fig. 6A). The optimized ball—and—stick models of BFA were presented in Fig. 6B. The average chemical formula was $C_{17}H_{16}O_7$ (Mr=332) in the BFA. Its main structure was composed of benzene rings, and its tetra— and fir—substituted. The large number of oxygen-containing functional groups in BFA, consisting of carboxyl and phenolic hydroxyl groups, had a high oxygen content. In addition, while most benzene rings were attached by methyl groups, lots of carboxyl groups situated at aliphatic carbon chains. This was agreed with the outcomes of the testing and instrumental analyses. It also discovered that different elements in BFA were similar to the experimental elemental analysis.

Gaussian software was used to calculate a theoretical FTIR spectrum for BFA, as shown in Fig. 6. The comparison of the experimental spectrum (Fig. 6D) and the calculated spectrum (Fig. 6C). The positions and intensities of the main characteristic peaks were found to be in good agreement. This indicated that the created molecular structure model matched well with the actual molecular structure model. There were a few differences in absorption peak intensities observed in the experimental spectrum of BFA. As an example, the experimental spectrum showed a broad and strong absorption peak in the range 1000–1500 cm^{-1}, mainly due to the vibrations of different types of oxygen-containing functional groups in the BFA. In the calculated spectrum, there was a comparatively broad absorption peak between 3000 cm^{-1} and 4000 cm^{-1}. Several small and sharp absorption peaks were found between 3500 cm^{-1} and 4000 cm^{-1}. The minor differences in these peak positions may be owing to the impact of hydrogen bonding on the spectral calculations (Yao et al., 2019b). In the calculated spectra, there were many sharp peaks, while the experimental spectra contained less and broader peaks. Being the large and broad absorption peaks, the potential reason was the superposition of multiple absorption peaks for everyone functional group in the experimental spectrum.

The calculated infrared spectrum highlights the typical peaks for each functional group in the molecular structure. The other parameters used to optimize the BFA model are presented in Table A.19–20. The BFA molecular structure exhibited a smaller molecular weight and more straightforward molecular structure than the MFA molecular structure (Gong et al., 2020). Specifically, the MFA molecular structure included one more nitrogen atom than BFA. The molecular weight of BFA was half that of MFA. Moreover, there were differences in the degree, number, and types of substitution. However, the benzene ring was the main component in the molecular structures of BFA and MFA (Gong et al., 2020).

In all, the functional groups of BFA and MFA were found to be similar, as shown in Fig. 6. However, the molecular weights of BFA and MFA were significantly different, which may be caused by the other extracting materials. Building molecular models of BFA at various molecular scales is useful for exploring the physicochemical properties of BFA.

3.5. *Rice seed germination*

Several studies have confirmed the efficacy and economic value of fulvic acid in agricultural production (Braziene et al., 2021). The root system plays a crucial role in plant growth, especially for nutrient uptake (Felizeter et al., 2014). Compared with the control group, 0.3% BFA and 0.5% MFA significantly increased the seed root length (Fig. 7A). The 0.4% BFA and 0.3% MFA treatments notably increased the fresh weights (Fig. 7B). The 0.2%—0.4% BFA, 0.1% MFA, 0.3% and 0.4% MFA treatments improved the seed germination rates from 50% to more than 60% (Fig. 7C). Similarly, using the fulvic acid for seed dressing, it increased the final germination percentage and reduced the mean germination time for spring wheat, spring barley, and sugar beet (Braziene et al., 2021). The MFA germination index at 0.4% was significantly different from that of the control group (Fig. 7D). The best treatment was that with 0.3% MFA and 0.4% BFA (Fig. 7E-F). BFA facilitated the growth of taproots and lateral roots. The same data showed that soaking the seeds with fulvic acid accelerated seed metabolism and promoted

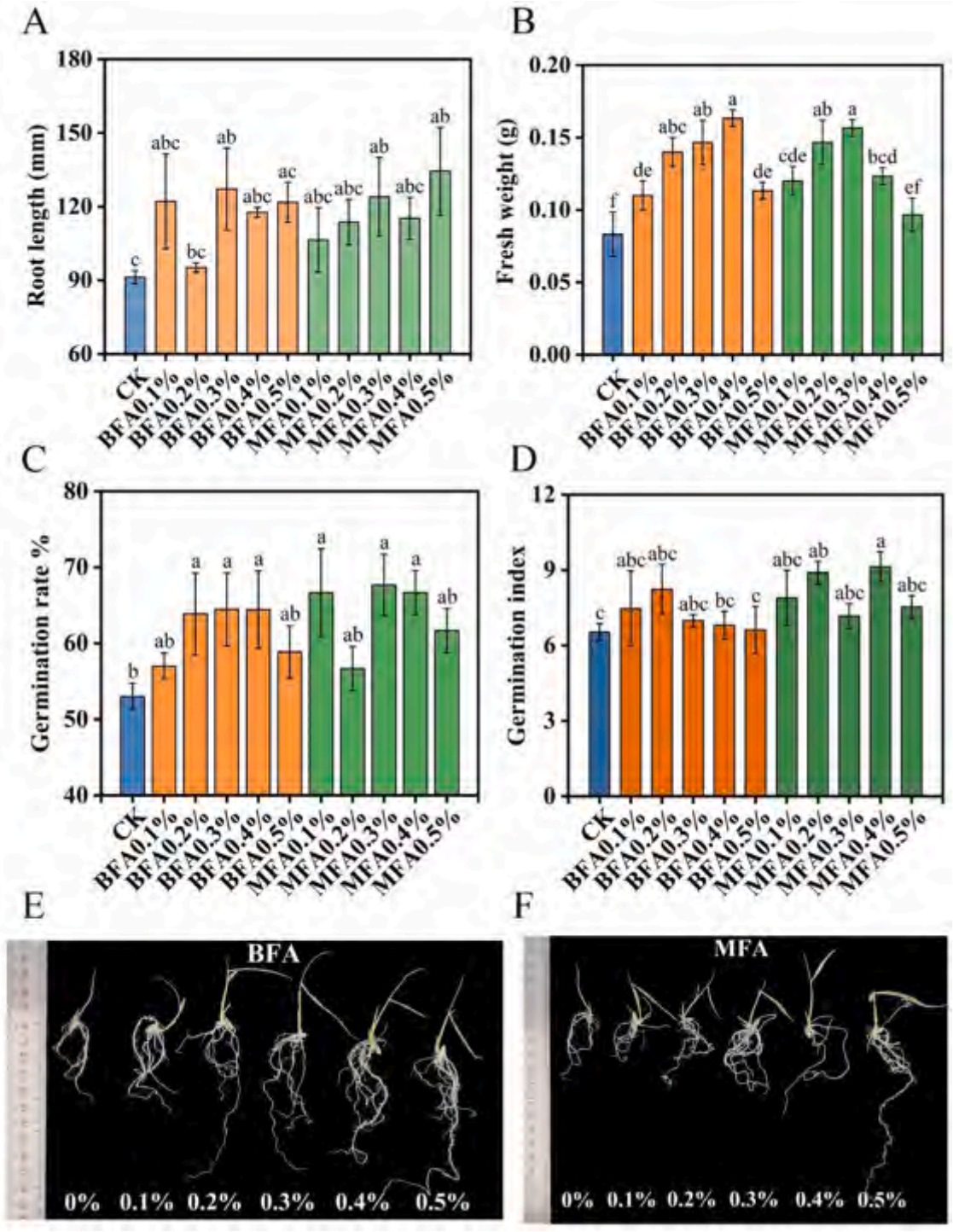

Fig. 7. Seed germination experiments with fulvic acid from corn straw compost. The seed germination rate (A), seed germination index (B), seed fresh weight (C), and seed root length (D) are shown for different treatments with BFA and MFA. Seed germination photos for rice with different proportions of BFA (E) and MFA (F). The results are the means of three replicates with error bars as the standard deviation. Lowercase letters represent significant differences between treatment groups.

seed rooting and germination (Wang et al., 2020). Straw extraction and microbial fermentation of fulvic acid enhanced the germination, production and yield of vegetables. A potential reason was that fulvic acid promoted the growth of lateral roots and increased the lengths of the main roots. As with plant hormones, heightened nutrient uptake is more likely due to auxin-like substances (Braziene et al., 2021; Wang et al., 2020; Zhang et al., 2021). BFA contained more oxygen—containing functional groups, which promoted oxidation—reduction reactions in the plants, thereby promoting plant growth. It was found that fulvic acid changed the root—to—shoot ratio and significantly increased the biomass, length, surface area, diameter, and volume of the roots (Wang et al., 2022). Under salt stress, PFA1–3 promoted the growth of rice (Yao et al., 2019a). Fulvic acid at 80 mg L^{-1} increased the seed germination rate by 12.9% and the radical length index and vigour index by 32.2% and 49.7%, respectively (Zhang et al., 2021). The effects of fulvic acid on plants depend on the source organic matter, the plant species, and the growth medium (Calvo et al., 2014). The use of humic acid (WHA), fulvic acid potassium (FAP), and fulvic acid distillate (FAD) improved

the quality of lemons to varying degrees (He et al., 2022). Adding fulvic acid effectively mitigated the combined effect of alkaline salt and freeze—thaw stresses on plants (Qu et al., 2022).

Based on the above data, BFA and MFA had similar effects. BFA is capable of use as a substitute for MFA, which has enormous application prospects in agriculture and other fields. It can also be used as a growth enhancer with specially coated microcapsules, which is vital for reducing the use of chemical fertilizers (Pour et al., 2022). The real industrial production conditions and methods will be optimized in subsequent investigations. Effective microbiological strains should also be used for the fulvic acid extraction process. A wide range of field experiments should be carried out to determine the dosage and ensure the stability of the product.

4. Conclusions

In this study, the best alkali solution acid precipitation extraction conditions were obtained, and the maximum extraction yield of fulvic acid reached 2.063 g/L. BFA and MFA had similar structures in the benzene ring as the major carbon skeleton in the molecular structure model. Both BFA and MFA significantly enhanced rice seed germination and root length. BFA could reduce the use of nonrenewable resources by replacing MFA. The results also provided a foundation for extracting fulvic acid from the corn straw compost in the industry. In the future, BFA could be used with fertilizer as a new functional synergistic fertilizer.

CRediT authorship contribution statement

Meisheng Chi: Conceptualization, Formal analysis, Writing – original draft. **Zhigang Wang**: Methodology, Formal analysis, Conceptualization, Supervision. **Weihui Xu**: Methodology, Writing – review & editing. **Ruixing Hou**: Writing – review & editing, Supervision.

Declaration of Competing Interest

The authors declare that they have no known competing financial interests or personal relationships that could have appeared to influence the work reported in this paper.

Data availability

The data that has been used is confidential.

Acknowledgement

Key Research and Development Program of Heilongjiang Province in China (GA21B007, GZ20210014 and GZ20210067), Pilot Project of the Chinese Academy of Sciences (XDA28130302) and Basic Scientific Research Funds for Colleges and Universities in Heilongjiang Province of China (145209805).

Appendix A. Supporting information

Supplementary data associated with this article can be found in the online version at doi:10.1016/j.indcrop.2023.116678.

References

Aida, A., Sana, A., Raouf, G., Hassene, A., 2022. Geochemistry of the Saouaf Formation lignite levels (Serravalian-Tortonian) in Zeramedine basin, central-eastern Tunisia. Arab. J. Geosci. 15, 1–26. https://doi.org/10.1007/s12517-022-10787-y.

Alberts, J.J., Takacs, M., 2004. Total luminescence spectra of IHSS standard and reference fulvic acids, humic acids and natural organic matter: comparison of aquatic and terrestrial source terms. Org. Geochem. 35, 243–256. https://doi.org/10.1016/j.orggeochem.2003.11.007.

Amir, S., Hafidi, M., Merlina, G., Hamdi, H., Revel, J.C., 2004. Elemental analysis, FTIR and C-13-NMR of humic acids from sewage sludge composting. Agronomie 24, 13–18. https://doi.org/10.1051/agro:2003054.

Amir, S., Hafidi, M., Merlina, G., Revel, J.C., 2005. Structural characterization of fulvic acids during composting of sewage sludge. Process Biochem 40, 1693–1700. https://doi.org/10.1016/j.procbio.2004.06.037.

Baddi, G.A., Hafidi, M., Cegarra, J., Alburquerque, J.A., Gonzalvez, J., Gilard, V., Revel, J.C., 2004. Characterization of fulvic acids by eleSmental and spectroscopic (FTIR and C-13-NMR) analyses during composting of olive mill wastes plus straw. Bioresour. Technol. 93, 285–290. https://doi.org/10.1016/j.biortech.2003.10.026.

Braziene, Z., Paltanavicius, V., Avizienyte, D., 2021. The influence of fulvic acid on spring cereals and sugar beets seed germination and plant productivity. Environ. Res. 195, 110824 https://doi.org/10.1016/j.envres.2021.110824.

Calvo, P., Nelson, L., Kloepper, J.W., 2014. Agricultural uses of plant biostimulants. Plant Soil 383, 3–41. https://doi.org/10.1007/s11104-014-2131-8.

Canellas, L.P., Olivares, F.L., Aguiar, N.O., Jones, D.L., Nebbioso, A., Mazzei, P., Piccolo, A., 2015. Humic and fulvic acids as biostimulants in horticulture. Sci. Hortic. -Amst. 196, 15–27. https://doi.org/10.1016/j.scienta.2015.09.013.

Cao, X.Y., Drosos, M., Leenheer, J.A., Mao, J.D., 2016. Secondary structures in a freeze-dried lignite humic acid fraction caused by hydrogen-bonding of acidic protons with aromatic rings. Environ. Sci. Technol. 50, 1663–1669. https://doi.org/10.1021/acs.est.5b02859.

Chang, Q., Lu, Z., He, M., Gao, R., Bai, H., Shi, B., Shan, A., 2014. Effects of dietary supplementation of fulvic acid on lipid metabolism of finishing pigs. J. Anim. Sci. 92, 4921–4926. https://doi.org/10.2527/jas.2014-8137.

Cornejo, A., Jimenez, J.M., Caballero, L., Melo, F., Maccioni, R.B., 2011. Fulvic acid inhibits aggregation and promotes disassembly of tau fibrils associated with alzheimer's disease. J. Alzheimers Dis. 27, 143–153. https://doi.org/10.3233/JAD-2011-110623.

Cusack, P., 2008. Effects of a dietary complex of humic and fulvic acids (FeedMAX 15 (TM)) on the health and production of feedlot cattle destined for the Australian domestic market. Aust. Vet. J. 86, 46–49. https://doi.org/10.1111/j.1751-0813.2007.00242.x.

Desbene, P.L., Silly, L., Morizur, J.P., Delamar, M., 1986. XPS Analysis of humic and fulvic-acids. Anal. Lett. 19, 2131–2140. https://doi.org/10.1080/00032718608080871.

Farzadnia, S., Nimmagadda, R.D., McRae, C., 2017. A comparative structural study of nitrogen-rich fulvic acids from various Antarctic lakes. Environ. Chem. 14, 502–514. https://doi.org/10.1071/EN17095.

Felizeter, S., McLachlan, M.S., De Voogt, P., 2014. Root uptake and trans location of perfluorinated alkyl acids by three hydroponically grown crops. J. Agr. Food Chem. 62, 3334–3342. https://doi.org/10.1021/jf500674j.

Francioso, O., Sanchez-Cortes, S., Tugnoli, V., Ciavatta, C., Gessa, C., 1998. Characterization of feat fulvic acid fractions by means of FT-IR, SERS, and H-1, C-13 NMR spectroscopy. Appl. Spectrosc. 52, 270–277. https://doi.org/10.1366/0003702981943347.

Fujitake, N., Tsuda, K., Aso, S., Kodama, H., Maruo, M., Yonebayashi, K., 2012. Seasonal characteristics of surface water fulvic acids from Lake Biwa and Lake Tankai in Japan. Limnology 13, 45–53. https://doi.org/10.1007/s10201-011-0354-4.

Gao, X.T., Tan, W.B., Zhao, Y., Wu, J.Q., Sun, Q.H., Qi, H.S., Xie, X.Y., Wei, Z.M., 2019. Diversity in the mechanisms of humin formation during composting with different materials. Environ. Sci. Technol. 53, 3653–3662. https://doi.org/10.1021/acs.est.8b06401.

Geng, J.B., Yang, X.Y., Huo, X.Q., Chen, J.Q., Lei, S.T., Li, H., Lang, Y., Liu, Q.J., 2020. Determination of the best controlled-release potassium chloride and fulvic acid rates for an optimum cotton yield and soil available potassium. Front. Plant Sci. 11, 562335 https://doi.org/10.3389/fpls.2020.562335.

Gerasimowicz, W.V., Byler, D.M., 1985. C-13 CPMAS NMR and FTIR spectroscopic studies of humic acids. Soil Sci. 139, 270–278. https://doi.org/10.1097/00010694-198503000-00013.

Gigliotti, G., Giusquiani, P.L., Businelli, D., 2001. A long-term chemical and infrared spectroscopy study on a soil amended with municipal sewage sludge. Agronomie 21, 169–178. https://doi.org/10.1051/agro:2001115.

Gondar, D., Lopez, R., Fiol, S., Antelo, J.M., Arce, F., 2005. Characterization and acid-base properties of fulvic and humic acids isolated from two horizons of an ombrotrophic peat bog. Geoderma 126, 367–374. https://doi.org/10.1016/j.geoderma.2004.10.006.

Gong, G.Q., Zhao, Y.F., Zhang, Y.J., Deng, B., Liu, W.X., Wang, M., Yuan, X., Xu, L.W., 2020. Establishment of a molecular structure model for classified products of coal-based fulvic acid. Fuel 267, 117210. https://doi.org/10.1016/j.fuel.2020.117210.

Gong, G.Q., Wang, Z.Y., Zhang, Y.J., Xu, W.X., Li, Z.L., Liang, S.J., Li, R.N., Lu, S., 2022a. Extraction of fulvic acid by citric acid-ethanol method and its biochemical activity. J. Chem. Technol. Biot. 97, 1259–1266. https://doi.org/10.1002/jctb.7020.

Gong, G.Q., Zhang, Y.J., Zheng, H.L., 2022b. Extraction and characterization of coal-based fulvic acid from Inner Mongolia lignite by hydrogen peroxide-glacial acetic acid. Chem. Pap. 76, 1665–1674. https://doi.org/10.1007/s11696-021-01986-0.

He, J.F., Zhu, L.T., Liu, C.G., Bai, Q., 2019. Optimization of the oil agglomeration for high-ash content coal slime based on design and analysis of response surface methodology (RSM. Fuel 254, 115560. https://doi.org/10.1016/j.fuel.2019.05.143.

He, X.Y., Zhang, H.Q., Li, J.X., Yang, F., Dai, W.F., Xiang, C., Zhang, M., 2022. The positive effects of humic/fulvic acid fertilizers on the quality of lemon fruits. Agron. -Basel 12, 1919. https://doi.org/10.3390/agronomy12081919.

Hernandez, M.T., Moreno, J.I., Costa, F., Gonzalezvila, F.J., Frund, R., 1990. Structural features of humic acidlike substances from sewage sludges. Soil Sci. 149, 63–68. https://doi.org/10.1097/00010694-199002000-00001.

Hiradate, S., Yonezawa, T., Takesako, H., 2006. Isolation and purification of hydrophilic fulvic acids by precipitation. Geoderma 132, 196–205. https://doi.org/10.1016/j.geoderma.2005.05.007.
Huculak-Maczka, M., Hoffmann, J., Hoffmann, K., 2018. Evaluation of the possibilities of using humic acids obtained from lignite in the production of commercial fertilizers. J. Soil Sediment 18, 2868–2880. https://doi.org/10.1007/s11368-017-1907-x.
Huguet, A., Vacher, L., Relexans, S., Saubusse, S., Froidefond, J.M., Parlanti, E., 2009. Properties of fluorescent dissolved organic matter in the Gironde Estuary. Org. Geochem. 40, 706–719. https://doi.org/10.1016/j.orggeochem.2009.03.002.
Iimura, Y., Ohtani, T., Chersich, S., Tani, M., Fujitake, N., 2012. Characterization of DAX-8 adsorbed soil fulvic acid fractions by various types of analyses. Soil Sci. Plant Nutr. 58, 404–415. https://doi.org/10.1080/00380768.2012.708318.
Inbar, Y., Hadar, Y., Chen, Y., 1992. Characterization of humic substances formed during the composting of solid-wastes from wineries. Sci. Total Environ. 113, 35–48. https://doi.org/10.1016/0048-9697(92)90015-K.
Jarukas, L., Ivanauskas, L., Kasparaviciene, G., Baranauskaite, J., Marksa, M., Bernatoniene, J., 2021. Determination of organic compounds, fulvic acid, humic acid, and humin in peat and sapropel alkalineextracts. Molecules 26, 2995. https://doi.org/10.3390/molecules26102995.
Javed, S., Kohli, K., Ali, M., 2013. Microwave-assisted extraction of fulvic acid from a solid dosage form: a statistical approach. J. Pharm. Innov. 8, 175–186. https://doi.org/10.1007/s12247-013-9157-y.
Jiang, T., Han, G.H., Zhang, Y.B., Li, G.H., Huang, Y.F., 2011. A further study on the interaction between one of organic active fractions of the MHA binder and iron ore surface. Int. J. Miner. Process 100, 172–178. https://doi.org/10.1016/j.minpro.2011.07.002.
Keeler, C., Maciel, G.E., 2003. Quantitation in the solid-state C-13 NMR analysis of soil and organic soil fractions. Anal. Chem. 75, 2421–2432. https://doi.org/10.1021/ac020679k.
Li, H., Li, Y., Li, C., 2013. Characterization of humic acids and fulvic acids derived from sewage sludge. Asian J. Chem. 25, 10087–10091. https://doi.org/10.14233/ajchem.2013.15162.
Li, J., Qu, J.H., Liu, H.J., Liu, R.P., Zhao, X., Hou, Y.N., 2008. Species transformation and structure variation of fulvic acid during ozonation. Sci. China, Ser. B 51, 373–378. https://doi.org/10.1007/s11426-008-0021-8.
Li, S.Y., Li, M., Wang, G.X., Sun, X.L., Xi, B.D., Hu, Z.Y., 2019. Compositional and chemical characteristics of dissolved organic matter in various types of cropped and natural Chinese soils. Chem. Biol. Technol. Agric. 6, 20. https://doi.org/10.1186/s40538-019-0158-z.
Li, Y., Bai, Y., Wei, D., Wang, W., Li, Y.M., Xue, H., Hu, Y., Cai, S.S., 2021. Fluorescence spectrum characteristics of fulvic acid in black soil under different ratios of organic-inorganic fertilizers combined application. Spectrosc. Spect. Anal. 41, 3518–3523. https://doi.org/10.3964/j.issn.1000-0593(2021)11-3518-06.
Lopez-Martinez, V.G., Guerrero-alvarez, J.A., Ronderos-Lara, J.G., Murillo-Tovar, M.A., Sola-Perez, J.E., Leon-Rivera, I., Saldarriaga-Norena, H., 2021. Spectral characteristics related to chemical substructures and structures indicative of organic precursors from fulvic acids in sediments by NMR and HPLC-ESI-MS. Molecules 26, 4051. https://doi.org/10.3390/molecules26134051.
Lu, Y.N., Ma, L.T., Li, J., 2021. Effects of sulfuric acid pretreatment and liquid acids precipitation on the structure of fulvic acid extracted from peat. Spectrosc. Lett. 54, 89–98. https://doi.org/10.1080/00387010.2020.1854306.
Lv, D., Sun, H., Zhang, M., Li, C., 2022. Fulvic acid fertilizer improves garlic yield and soil nutrient status. Gesund Pflanz. 74, 685–693. https://doi.org/10.1007/s10343-022-00644-z.
Ma, L.T., Lu, Y.N., Wang, Y.X., 2020. Effects of methane fermentation on spectral properties of fulvic acid extracted from peat through liquid acid precipitation. J. Chem. -Ny. 2020. https://doi.org/10.1155/2020/5084508.
Martinez-Balmori, D., Spaccini, R., Aguiar, N.O., Novotny, E.H., Olivares, F.L., Canellasa, L.P., 2014. Molecular characteristics of humic acids isolated from vermicomposts and their relationship to bioactivity. J. Agr. Food Chem. 62, 11412–11419. https://doi.org/10.1021/jf504629c.
May, L., 1965. Introduction to practical infrared spectroscopy. Appl. Spectrosc. 19, 62–76.
Mghaiouini, R., Benzibiria, N., Monkade, M., Bouari, A.E., 2022. Formulation of new biostimulant of plant and soil correction based on humic acids extracted by magnetized water from compost from the waste of coffee marc and cattle manure. Waste Biomass-.-. Valor 13, 453–465. https://doi.org/10.1007/s12649-021-01535-6.
Nargesi, M.M., Sedaghathoor, S., Hashemabadi, D., 2022. Effect of foliar application of amino acid, humic acid and fulvic acid on the oil content and quality of olive. Saudi. J. Biol. Sci. 29, 3473–3481. https://doi.org/10.1016/j.sjbs.2022.02.034.
Peuravuori, J., Pihlaja, K., 1997. Molecular size distribution and spectroscopic properties of aquatic humic substances. Anal. Chim. Acta 337, 133–149. https://doi.org/10.1016/S0003-2670(96)00412-6.
Pour, M.M., Saberi-Riseh, R., Esmaeilzadeh-Salestani, K., Mohammadinejad, R., Loit, E., 2021. Evaluation of bacillus velezensis for biological control of rhizoctonia solani in bean by alginate/gelatin encapsulation supplemented with nanoparticles. J. Microbiol Biotechn 31, 1373–1382. https://doi.org/10.4014/jmb.2105.05001.
Pour, M.M., Riseh, R.S., Ranjbar-Karimi, R., Hassanisaadi, M., Rahdar, A., Baino, F., 2022. Microencapsulation of bacillus velezensis using alginate-gum polymers enriched with TiO2 and SiO2 nanoparticles. Micromachines 13, 1423. https://doi.org/10.3390/mi13091423.
Preston, C.M., 1996. Applications of NMR to soil organic matter analysis: History and prospects. Soil Sci. 161, 144–166. https://doi.org/10.1097/00010694-199603000-00002.
Qu, Y., Bao, G.Z., Pan, X.Y., Guo, J.C., Xiang, T., Fan, X.Y., Zhang, X., Yang, Y.A., Yan, B. R., Zhao, H.W., Li, G.M., 2022. Resistance of highland barley seedlings to alkaline salt and freeze-thaw stress with the addition of potassium fulvic acid. Plant Soil Environ. 68, 299–308. https://doi.org/10.17221/84/2022-PSE.
Ricca, G., Severini, F., 1993. Structural investigations of humic substances by FTIR, C-13-NMR spectroscopy and comparison with a maleic oligomer of known structure. Geoderma 58, 233–244. https://doi.org/10.1016/0016-7061(93)90044-L.
Riseh, R.S., Pour, M.M., 2021. A novel encapsulation of Streptomyces fulvissimus Uts22 by spray drying and its biocontrol efficiency against gaeumannomyces graminis, the causal agent of take-all disease in wheat. Pest Manag Sci. 77, 4357–4364. https://doi.org/10.1002/ps.6469.
Riseh, R.S., Ebrahimi-Zarandi, M., Vazvani, M.G., Skorik, Y.A., 2021a. Reducing drought stress in plants by encapsulating plant growth-promoting bacteria with polysaccharides. Int J. Mol. Sci. 22, 12979. https://doi.org/10.3390/ijms222312979.
Riseh, R.S., Skorik, Y.A., Thakur, V.K., Pour, M.M., Tamanadar, E., Noghabi, S.S., 2021b. Encapsulation of plant biocontrol bacteria with alginate as a main polymer material. Int J. Mol. Sci. 22, 11165. https://doi.org/10.3390/ijms222011165.
Riseh, R.S., Hassanisaadi, M., Vatankhah, M., Babaki, S.A., Barka, E.A., 2022a. Chitosan as a potential natural compound to manage plant diseases. Int J. Biol. Macromol. 220, 998–1009. https://doi.org/10.1016/j.ijbiomac.2022.08.109.
Riseh, R.S., Tamanadar, E., Hajabdollahi, N., Vatankhah, M., Thakur, V.K., Skorik, Y.A., 2022b. Chitosan microencapsulation of rhizobacteria for biological control of plant pests and diseases: recent advances and applications. Rhizosphere 23, 100565. https://doi.org/10.1016/j.rhisph.2022.100565.
Shahid, M., Dumat, C., Silvestre, J., Pinelli, E., 2012. Effect of fulvic acids on lead-induced oxidative stress to metal sensitive Vicia faba L. plant. Biol. Fert. Soil. 48, 689–697. https://doi.org/10.1007/s00374-012-0662-9.
Sharma, A., Anthal, R., 2022. Fulvic acid isolation and characterisation from water of a Ramsar Lake Mansar, J&K, India. Appl. Water Sci. 12, 1–7. https://doi.org/10.1007/s13201-021-01536-9.
Shi, W., Fang, X.M., Wu, X.F., Zhang, G.X., Que, W.Y., Li, F.L., 2018. Alteration of bioaccumulation mechanisms of Cu by microalgae in the presence of natural fulvic acids. Chemosphere 211, 717–725. https://doi.org/10.1016/j.chemosphere.2018.07.200.
Shinozuka, T., Ito, A., Sasaki, O., Yazawa, Y., Yamaguchi, T., 2002. Preparation of fulvic acid and low-molecular organic acids by oxidation of weathered coal humic acid. Nippon Kagaku Kaishi 3, 345–350. https://doi.org/10.1246/nikkashi.2002.345.
Sitnichenko, T.N., Vakulenko, V.F., Goncharuk, V.V., 2011. Photocatalytic destruction of fulvic acids by oxygen in the TiO_2 suspension. J. Water Chem. Techno 33, 236–247. https://doi.org/10.3103/S1063455×11040059.
Sun, Y.P., Yang, J.S., Yao, R.J., Chen, X.B., Wang, X.P., 2020. Biochar and fulvic acid amendments mitigate negative effects of coastal saline soil and improve crop yields in a three year field trial. Sci. Rep. -Uk 10, 1–12. https://doi.org/10.1038/s41598-020-65730-6.
The Statista GmbH, 2007, Johannes-Brahms-Platz 1, Hamburg, Germany. https://www.statista.com/statistics/1156213/global-corn-production/ (accessed 22 November 2022).
Volk, C., Roche, P., Joret, J.C., Paillard, H., 1997. Comparison of the effect of ozone, ozone-hydrogen peroxide system and catalytic ozone on the biodegradable organic matter of a fulvic acid solution. Water Res 31, 650–656. https://doi.org/10.1016/S0043-1354(96)00302-8.
Wang, S., Huang, X.L., Zhang, Y., Yin, C.B., Richel, A., 2021. The effect of corn straw return on corn production in Northeast China: An integrated regional evaluation with meta-analysis and system dynamics. Resour. Conserv. Recy. 167, 105402 https://doi.org/10.1016/j.resconrec.2021.105402.
Wang, W.T., Zhen, W.J., Bian, S.Z., Xi, X., 2015. Structure and properties of quaternary fulvic acid-intercalated saponite/poly (lactic acid) nanocomposites. Appl. Clay Sci. 109, 136–142. https://doi.org/10.1016/j.clay.2015.02.033.
Wang, Y., Liu, Z.Q., Xiemuxiding, A., Zhang, X.F., Duan, L.S., Li, R.Z., 2022. Fulvic acid, brassinolide, and uniconazole mediated regulation of morphological and physiological traits in maize seedlings under water stress. J. Plant Growth Regul. 10658, 1–13. https://doi.org/10.1007/s00344-022-10658-6.
Wang, Z.H., Shen, T.L., Yang, Y.C., Gao, B., Wan, Y.S., Li, Y., Yao, Y.Y., Liu, L., Tang, Y.F., Xie, J.Z., Ding, F.J., Chen, J.Q., 2020. Fulvic acid-like substance and its characteristics, an innovative waste recycling material from pulp black liquor. J. Clean. Prod. 243, 118585 https://doi.org/10.1016/j.jclepro.2019.118585.
Winkler, J., Ghosh, S., 2018. Therapeutic potential of fulvic acid in chronic inflammatory diseases and diabetes. J. Diabetes Res 2018, 1–7. https://doi.org/10.1155/2018/5391014.
Yang, F., Zhang, S.S., Cheng, K., Antonietti, M., 2019. A hydrothermal process to turn waste biomass into artificial fulvic and humic acids for soil remediation. Sci. Total Environ. 686, 1140–1151. https://doi.org/10.1016/j.scitotenv.2019.06.045.
Yang, Y.H., Sheng, F.L., Tao, Z.Y., 2008. Transmission ftir difference spectroscopic characterization of a fulvic acid from weathered coal in water. Toxicol. Environ. Chem. 51, 135–144. https://doi.org/10.1080/02772249509358231.
Yao, Y.Y., Wang, C., Wang, X.Q., Yang, Y.C., Wan, Y.S., Chen, J.Q., Ding, F.J., Tang, Y.F., Wang, Z.H., Liu, L., Xie, J.Z., Gao, B., Li, Y., Sigua, G.C., 2019a. Activation of fulvic acid-like in paper mill effluents using H_2O_2/TiO_2 catalytic oxidation: Characterization and salt stress bioassays. J. Hazard Mater. 378, 120702 https://doi.org/10.1016/j.jhazmat.2019.05.095.
Yao, Y.Y., Wang, X.Q., Yang, Y.C., Shen, T.L., Wang, C., Tang, Y.F., Wang, Z.H., Xie, J.Z., Liu, L., Hou, S.M., Gao, B., Li, Y., Wan, Y.S., 2019b. Molecular composition of size-fractionated fulvic acid-like substances extracted from spent cooking liquor and its relationship with biological activity. Environ. Sci. Technol. 53, 14752–14760. https://doi.org/10.1021/acs.est.9b02359.

Zang, Z.R., Shi, W.J., Ma, H., Zhou, B., Li, H., Lu, C.W., He, J., 2020. Binding mechanism between fulvic acid and heavy metals: integrated interpretation of binding experiments, fraction characterizations, and models. Water Air Soil Poll. 231, 1–12. https://doi.org/10.1007/s11270-020-04558-2.

Zhang, A., Zhang, Y.J., Zheng, H.L., Ma, L.L., Liu, W.J., Gong, G.Q., 2018b. Study on the extraction of fulvic acid from lignite by microwave-assisted hydrogen peroxide. Int J. Oil Gas. Coal T 18, 146–162. https://doi.org/10.1504/IJOGCT.2018.091557.

Zhang, P.J., Zhang, H.J., Wu, G.Q., Chen, X.Y., Gruda, N., Li, X., Dong, J.L., Duan, Z.Q., 2021. Dose-dependent application of straw-derived fulvic acid on yield and quality of tomato plants grown in a greenhouse. Front. Plant Sci. 12, 736613 https://doi.org/10.3389/fpls.2021.736613.

Zhang, Y.J., Liu, W.J., Hu, X.F., Zhang, A., Ma, L.L., Shi, Y.M., Gong, G.Q., 2019. Extraction and functional group characterization of fulvic acid from hami lignite. Chemistryselect 4, 1448–1455. https://doi.org/10.1002/slct.201803291.

Zhang, Y.Y., Zong, Z.M., Sun, Y.B., Liu, F.J., Li, W.T., Wang, Y.N., Wei, X.Y., 2018a. Investigation on the structural feature of Shengli lignite. Int J. Min. Sci. Technol. 28, 335–342. https://doi.org/10.1016/j.ijmst.2017.05.022.